Chinese Journal of Chemical Engineering 73 (2024) 202–211

Contents lists available at ScienceDirect

Chinese Journal of Chemical Engineering

journal homepage: www.elsevier.com/locate/CJChE

Full Length Article

Effect of copper content on the pyrolysis process of organic components in waste printed circuit boards: Based on experimental and quantum chemical DFT simulations

Bin Li [1, 2], Biqin Shen [1, 2], Ran Tao [1, 2], Chenwei Hu [1, 2], Yufeng Wu [1, 2, *], Haoran Yuan [3], Jing Gu [3], Yong Chen [3]

[1] Institute of Circular Economy, Beijing University of Technology, Beijing 100124, China
[2] Faculty of Materials and Manufacturing, Beijing University of Technology, Beijing 100124, China
[3] Guangzhou Institute of Energy Conversion, Chinese Academy of Sciences, Guangzhou 510640, China

ARTICLE INFO

Article history:
Received 25 February 2024
Received in revised form
10 April 2024
Accepted 15 April 2024
Available online 8 June 2024

Keywords:
Waste printed circuit boards
Copper
Pyrolysis
Kinetic study
Density functional theory (DFT)

ABSTRACT

In recent years, scientists have become increasingly concerned in recycling electronic trash, particularly waste printed circuit boards (WPCBs). Previous research has indicated that the presence of Cu impacts the pyrolysis of WPCBs. However, there may be errors in the experimental results, as printed circuit boards (PCBs) with copper and those without copper are produced differently. For this experiment, we blended copper powder with PCB nonmetallic resin powder in various ratios to create the samples. The apparent kinetics and pyrolysis properties of four resin powders with varying copper concentrations were compared using nonisothermal thermogravimetric analysis (TG) and thermal pyrolysis-gas chromatography mass spectrometry (Py-GC/MS). From the perspective of kinetics, the apparent activation energy of the resin powder in the pyrolysis reaction shows a rise ($0.1 < \alpha < 0.2$)-stable ($0.2 < \alpha < 0.4$)-accelerated increase ($0.4 < \alpha < 0.8$)- decrease ($0.8 < \alpha < 0.9$) process. After adding copper powder, the apparent activation energy changes more obviously when ($0.2 < \alpha < 0.4$). In the early stage of the pyrolysis reaction ($0.1 < \alpha < 0.6$), the apparent activation energy is reduced, but when $\alpha = 0.8$, it is much higher than that of the resin sample without copper. Additionally, it is discovered using thermogravimetric analysis and Py-GC/MS that copper shortens the temperature range of the primary pyrolysis reaction and prevents the creation of compounds containing bromine. This inhibition will raise the temperature at which compounds containing bromine first form, and it will keep rising as the copper level rises. The majority of the circuit board molecules have lower bond energies when copper is present, according to calculations performed using the Gaussian09 software, which promotes the pyrolysis reaction.

1. Introduction

According to estimates by the United Nations (UN), the global e-waste production rate is increasing at a rate of 10% per year. Today, global annual e-waste production has exceeded 50 million tons [1]. E-waste production is expected to increase by 74.7 million tonnes by 2030 [2]. Printed circuit boards (PCBs) are not only the core component of electronic products and equipment but also the foundation of the electronics industry and the information industry [3]. They can be important carriers of various electronic components (such as chips, integrated circuits, resistors, and capacitors and are used to realize the interconnection between electronic components [4]. However, due to factors such as its own performance degradation and the replacement of electronic components, PCBs face many periodic scrapping problems. According to statistics, the number of waste printed circuit boards (WPCBs) in 2019 has reached 3 million tons and will continue to increase in the next ten years [5]. PCBs are composed of metal components and nonmetal components. Nonmetal components mainly include resin, glass fiber, and additives [6]. Due to the importance of metal resources to the development of a circular economy, current research on the recycling of WPCBs mainly focuses on metal components, and less attention is given to nonmetallic components [7].

* Corresponding author at: Tel.: +86 10 67396234; Fax: +86 10 67396234.
E-mail address: wuyufeng3r@126.com (Y. Wu).

https://doi.org/10.1016/j.cjche.2024.04.024

The recovery of valuable materials from organic solid waste through pyrolysis is considered to be an economical, environmentally friendly and promising method [8–10]. After removing the electronic components, WPCB can be decomposed into solid residue, liquid and gas products through pyrolysis in an inert atmosphere [11–13]. The current research on WPCB pyrolysis mainly focuses on mechanism analysis, kinetic analysis, and product analysis. Li *et al.* [14] found that pyrolysis removed bromine from the solid-phase product, while copper was effectively enriched. Ortuño *et al.* [15] studied the effect of the heating rate on pyrolysis products and found that at the same temperature, reducing the heating rate and extending the reaction time can increase the pyrolysis conversion rate. Du *et al.* [16] found that reducing the particle size of waste circuit board substrates can also increase the reaction rate. In addition, Du *et al.* [17] established a mathematical model and simulated the heat transfer process of pyrolysis. Through these analyses, the influence law of specific heat, thermal conductivity and reaction heat on the temperature distribution of the waste circuit board pyrolysis process is obtained. Chiang *et al.* [18] analyzed the influence of different pyrolysis conditions on the reaction products. The obtained results showed that temperature was the most critical factor affecting pyrolysis products. Zhao *et al.* [19] studied the effects of several molecular sieve catalysts on the pyrolysis process of waste PCBs and found that the ZSM-5 catalyst had a greater effect on the optimization of the pyrolysis process. However, although the pyrolysis process of WPCB is constantly being optimized, the pyrolysis oil and gaseous products contain a large number of organic and inorganic brominated compounds, which makes it difficult to solve the problem of the recovery and utilization of pyrolysis oil and gas and equipment exhaust emissions [20]. Therefore, ways to effectively reduce the bromine content in pyrolysis oil and gas has become a hot research direction.

To reduce the bromine content in pyrolysis oil and gas, several scientists have conducted research on reaction equipment and reagents [21]. Li *et al.* [22] used water vapor-assisted pyrolysis and found that about 94% (mass) of the bromine was transferred to water, reducing the production of bromination products and toxic substances. Wang *et al.* [23] used ball milling to pretreat WPCBs with metal oxide powders. The combined effect of mechanical energy and metal oxide can promote the transfer of bromine in WPCBs from the inside to the surface. Zhang *et al.* [24] used a microwave-assisted method for the pyrolysis of WPCBs. The obtained results showed that the debromination efficiency of adding K_2CO_3 and Na_2CO_3 under the assistance of microwaves was higher than 99%. Zhu *et al.* [25] used low-temperature vacuum pyrolysis to vacuum pyrolyze WPCB particles at a low temperature of 300 °C so that most of Br on the resin molecule was transferred to the pyrolysis oil without destroying the partial resin integrity. Ma and Kamo [26] used Fe and Ni as catalysts to participate in the pyrolysis reaction of WPCBs. The obtained results showed that iron powder could successfully reduce the concentration of brominated compounds in the oil produced, especially for organic brominated compounds. Terakado *et al.* [27] selected some metal oxides, including zinc oxide, calcium oxide, and lanthanum oxide, as catalysts to fix the release of bromine during the pyrolysis of WPCBs. The main principle is to fix the generated HBr by brominating the metal oxides. The test results show that zinc oxide and lanthanum oxide have a better bromine-fixing effect, and calcium dioxide's bromine-fixing effect is weaker than expected. Whether copper, which has the highest content in WPCBs, will have a certain effect on pyrolysis and debromination reactions has been discussed in individual experiments in recent years. Gao *et al.* [28] determined that the coexistence of Cu metal can reduce the activation energy of the pyrolysis reaction of WPCBs. This is also conducive to inhibiting the generation of bromine-containing organics and promoting the generation of Br_2 and HBr, thereby reducing the difficulty of recovery and treatment of pyrolysis oil. Liu *et al.* [29] discussed the reaction mechanism of the pyrolysis of copper-containing and copper-free circuit boards. They believed that the presence of copper promoted the reaction and reduced the generation of carbonyl compounds and brominated compounds, but it also increased the difficulty of exhaust gas treatment. From this point of view, the presence of copper will have a greater impact on the pyrolysis reaction of WPCBs. Whether it is necessary to separate the metal and nonmetal parts during the pretreatment of WPCBs is not yet a definite conclusion. Therefore, it is necessary to explore the influence of copper content on the pyrolysis of nonmetallic components of circuit boards.

This experiment combines thermogravimetry-derivative thermogravimetry (TG-DTG), kinetic analysis, and pyrolysis-gas chromatography-mass spectrometry (Py-GC/MS) to explore the effect of copper content on the pyrolysis of nonmetallic components of the circuit board. The differences in pyrolysis behavior were compared through the TG-DTG test results. The kinetics adopts the Flynn-Wall-Ozawa model and compares the difference between the activation energy of the reaction and the pre-explicit factor *A* under several different copper content conditions. Py-GC/MS was used to monitor the gas products in different heating intervals and analyze the influence of copper content on the product formation. Finally, according to calculations using the Gaussian09 software, copper enhances the pyrolysis reaction by lowering the binding energies of the majority of the circuit board molecules.

2. Materials and Method

2.1. Materials

The resin powder with different copper contents used in the experiment was made by mixing resin powder and copper powder. The copper content of the four samples was 0%, 15%, 30% and 45%. Resin Powder is a non-metallic resin powder obtained by removing, physically pulverizing, sorting, and sieving the electronic components from Boston brand 4G memory sticks through a 200 mesh (0.075 mm) screen. It comes from a resource recycling technology company in Changzhou, Jiangsu. Its main components are polyester resin, brominated epoxy resin, glass fiber powder, phosphorus-containing flame retardants, and nitrogen-containing hardeners. The fine copper powder comes from a technology company in Beijing. To mix the copper powder and the resin powder uniformly, a ball mill was used to continue grinding for 4 h after the sample configuration was completed so that the two powders were fully mixed to form the experimental sample.

The contents of carbon, hydrogen, oxygen, nitrogen, and sulfur in the resin powder were determined by an elemental analyzer (vario MACRO). After testing three times, the average value was taken as the final element content. A calorimeter was used to fully burn the resin powder placed in it under oxygen-filled conditions. The bromine element is converted into hydrogen bromide gas and absorbed by the NaOH absorption liquid in the oxygen bomb. Then, the content of bromide ions was detected by ion chromatography to calculate the content of bromine in the original test sample. The copper content in the resin sample was obtained by ICP.

The ultimate analysis results of the resin sample are shown in Table 1.

Table 1
Ultimate analysis of resin samples (%)

C	H	O	N	S	Br	Cu
28.53	2.92	12.71	1.37	0.311	4.823	0.23

2.2. Infrared spectral analysis of resin powder samples

The functional groups contained in the resin sample were analyzed by an infrared spectrum analyzer (IRAffinity). The obtained infrared spectrum is shown in Fig. 1. It can be seen from the curve in Fig. 1 that there is a strong and broad absorption peak at 3454 cm^{-1}, which is the overlap range of the physical water absorption peak and the hydroxyl absorption peak of the sample. Since the sample preparation under the infrared drying lamp reduces the influence of water absorption of the sample, it is mainly caused by the —OH stretching vibration in the sample [30]. The absorption peak at 2919 cm^{-1} is caused by the symmetric stretching vibration of the benzene ring directly connected to the methyl CH; the absorption peak at 2385 cm^{-1} is caused by the stretching vibration of Si—H formed by SiO_2 in the glass fiber and —OH in the resin [31]. The peak at 1729 cm^{-1} is the stretching vibration peak of —C=O, and it may also be the stretching vibration peak of —C=O in the free carboxylic acid. This result indicates that there are carbonyl or carboxyl groups in the sample. The three absorption peaks between 1396 cm^{-1} and 1604 cm^{-1} are the characteristic peaks of aromatic hydrocarbons. The benzene ring skeleton C=C stretches exhibit peaks in this region. The absorption peak at 1241 cm^{-1} is the C—O(H) stretching vibration peak, indicating that the sample contains hydroxyl groups. The 1029 cm^{-1} peak is in the C—O—C stretching vibration zone. This result confirms the presence of an epoxy structure in the sample. The absorption peak at 751 cm^{-1} is the C—H stretching vibration peak on the benzene ring. The stretching vibration peaks at 480 cm^{-1} and 622 cm^{-1} are the absorption peaks of the C—Br bond, indicating that the sample contains bromine [32]. The double peaks may be due to the difference in the amount of —Br on different benzene rings. Generally, the greater the substitution number, the higher the wavenumber.

2.3. Parameters of the pyrolysis process

Under nitrogen atmosphere, thermogravimetric analysis was used to study and discuss the pyrolysis characteristics and reaction kinetics of the sample powder. The TG/DTA thermogravimetric/differential thermal integrated analyzer (labsys evo) used was obtained from the instrument sharing platform of Beijing University of Technology. The temperature accuracy was 0.01 °C, the heating rate was 0.1–40 °C·min^{-1}, the thermobalance accuracy was 0.1 μg, the injection volume was approximately 5–20 mgeach time, the atmosphere was nitrogen, and the flow rate was 30 ml·min^{-1}. The temperature rise rate of the sample powder was set to 10, 20 and 30 °C·min^{-1}, and the temperature measurement range was from room temperature to 800 °C.

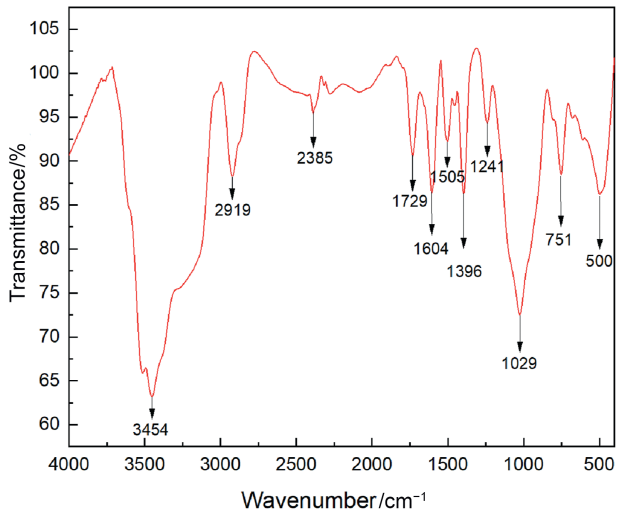

Fig. 1. FT-IR spectrum of the resin powder sample.

The Py-GC/MS experiment was designed based on the sample reaction temperature obtained by thermogravimetric analysis. Using mass spectrometry results and organic chemical reaction theory, the formation mechanism of samples under different temperature intervals and different copper contents can be inferred. The fast pyrolysis of samples was performed in an analytical CDS Pyroprobe 5200 pyrolyzer coupled with gas chromatography/mass spectrometry (Agilent 7890A/5977A). An Agilent DB-1701 column (length, 60 m; inner diameter, 0.25 mm; film thickness, 0.25 μm) was used in this experiment. Approximately 0.10–0.20 mg of the sample was placed into a quartz tube, and then the pyrolysis gas species were transferred into GC/MS for characterization. The experiment was performed at a heating rate of 20 °C·ms^{-1} at 480 °C; the carrier gas was high-purity helium, and the dwell sampling temperatures were 230, 280, 330, 380, 430 and 480 °C. The GC oven temperature was first set at 40 °C for 4 min, then heated to 230 °C with a heating rate of 5 °C·min^{-1} and finally held at 230 °C for 5 min. Electron ionization was set at 70 eV, and the range of analysis of the mass spectrometer was 30–500 *m*/*z*. The MS spectra were identified based on the mass spectral library (NIST 14).

3. Results and Discussion

3.1. TG and DTG analysis

Figs. 2 and 3 show the TG, DTG, and D^2TG curves of four resin powders with different copper contents in a nitrogen atmosphere heated from room temperature to 800 °C at heating rates of 10, 20, and 30 °C·min^{-1}. It can be seen from the TG curve that the heating rate has little effect on the pyrolysis reaction of the resin powder sample, and there is no significant difference in the mass loss rate of the samples under three different heating rates. From the DTG curve, we can see that as the heating rate increases, the maximum mass loss peak of the curve moves to higher temperature, and the peak value significantly increases. The maximum mass loss rate is also increased. However, the position of the maximum mass loss peak coincides with the curve of the higher heating rate, indicating that the change in the heating rate does not affect the initial reaction temperature of the pyrolysis of the resin powder.

Fig. 3 shows the D^2TG curve of the sample, which was obtained by redifferentiation of the DTG curve. From the D^2TG curve, the pyrolysis reaction interval, maximum peak temperature and maximum mass loss rate of four samples with different copper contents can be derived. From Table 2, the pyrolysis characteristics of four samples with different copper contents can be seen. Their main reaction temperature is 250–500 °C, and there are 3 reaction zones and 2 transition zones. The boundary range of the interval increases with increasing heating rate. The first reaction interval is 220–280 °C, and the mass loss is approximately 6%, mainly due to the volatilization of low boiling point compounds and the removal of macromolecular organic side chains such as HBr and H_2O. The first transitional interval is between 280 °C and 350 °C, which manifests as the overlap and conversion of the two-stage reactions. The volatilization of low-boiling point compounds continues, and the process of removing macromolecular side chains tends to end. The zero point in the D^2TG curve indicates that the turning point of the reaction occurred near 350 °C. This represents the beginning of a new cleavage reaction. The second reaction interval is 350–480 °C, which is the main reaction interval for the cleavage of organic matter in the sample. The total mass loss of the sample in this interval is approximately 22%. The main reaction is the rupture of the brominated epoxy resin structure and the release of high-boiling volatiles from the cracking process.

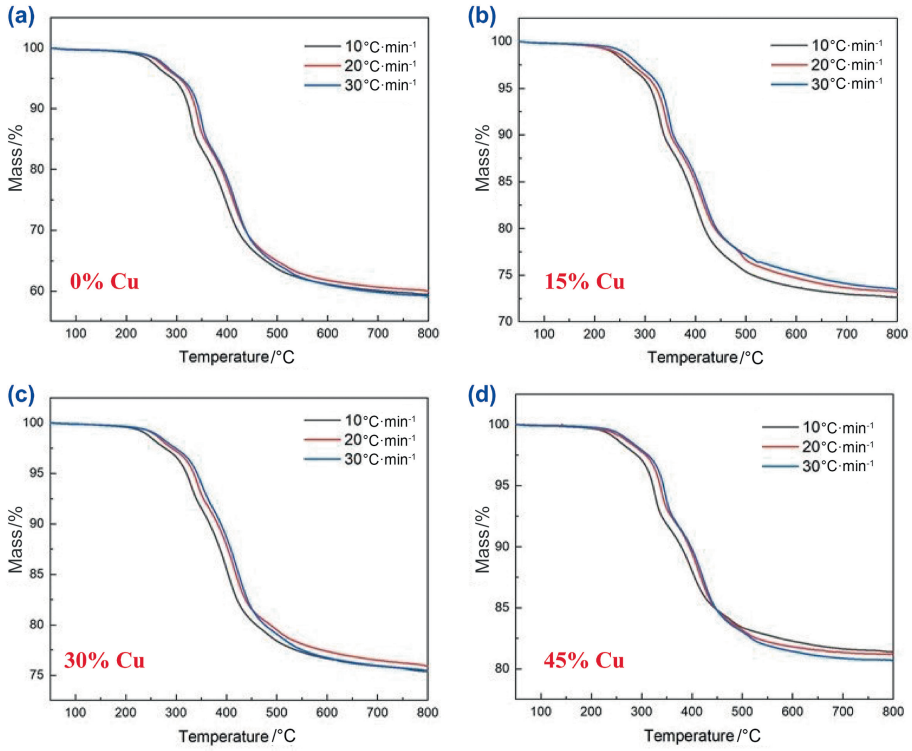

Fig. 2. TG curves of four resin powders with different copper contents: (a) resin powder without copper, (b) resin powder with a 15% copper mass fraction, (c) resin powder with a 30% copper mass fraction, and (d) resin powder with a 45% copper mass fraction.

This reaction is accompanied by the dehydration and volatilization of high boiling point macromolecules, leading to rapid mass loss in the reaction interval. The data in Fig. 3 shows that the temperature range of the second reaction zone of the copper-containing resin powder is significantly reduced, indicating that the presence of copper will shorten the main reaction zone in the resin pyrolysis process and that copper may play a catalytic role in the pyrolysis process of the resin. The second transitional interval is 480–520 °C. At the beginning of this interval, the cracking process of resin macromolecules tended to end. In the DTG curve, the rapid decline in the mass loss rate begins to stabilize, and the value is similar to the mass loss rate in the first reaction interval. At this stage, the volatilization of low boiling point compounds continues. However, the rate of mass loss at the end of this stage decreased, indicating that the volatilization of low-boiling volatiles in the second transition zone also tended to end. The third reaction interval is 520–800 °C, and the mass loss rate is relatively stable. The main reaction in this stage is the deep carbonization of residual carbon and the continuous escape of some residual small molecules. Although the third reaction interval exists, it can be seen that the total mass loss rate and mass loss rate in this interval are very low and tend to zero. This shows that the pyrolysis reaction of the resin powder was basically completed in the second reaction zone and the second transition zone. In other words, the resin powder almost completely pyrolyzed macromolecules at 520 °C, and the subsequent heating process did not greatly improve the pyrolysis efficiency of the resin powder. Most likely due to this reason, in recent years, research on whether resin-containing solid waste can be pyrolyzed at lower temperature has gradually increased.

3.2. Kinetics analysis

In this study, the Flynn-Wall-Ozawa (FWO) model was used to calculate the apparent activation energy of the sample. The FWO model is currently a more mature method in the calculation of complex thermal reaction models [33]. The temperature integral approximation formula obtained by the FWO method avoids the choice of the reaction mechanism function and directly calculates the activation energy of the reaction. The omission of this high-order formula avoids the problem of solving the pyrolysis model due to the difference in the choice of the reaction mechanism function [34]. Studies have shown that the results obtained using traditional temperature integral expressions and numerical calculations are quite different [35].

We can express the total reaction equation of the pyrolysis of the resin powder as:

$$\mathrm{A(solid)} \rightarrow \mathrm{B(solid)} + \mathrm{C(gas)} \tag{1}$$

where A is the reactant, and B with C is the product of pyrolysis.

According to the law of mass action:

$$\frac{\mathrm{d}\alpha}{\mathrm{d}t} = kf(\alpha) \tag{2}$$

where α is the sample conversion fraction, the expression is $\alpha = (m_0 - m_1)/(m_0 - m_2)$, m_0 is the initial mass of the sample, m_1 is the process mass of the sample, and m_2 is the final mass of the sample.

According to Arrhenius equation:

$$k = A\ \exp\left(-\frac{E_a}{RT}\right) \tag{3}$$

where A is the pre-exponential factor, R is the mole gas constant, with a value of 8.314 $\mathrm{J\cdot mol^{-1}\cdot K^{-1}}$, T is the thermodynamic temperature, E_a is the apparent activation energy, and k is the rate constant.

By substituting Eq. (3) into (2), we can obtain the following equation:

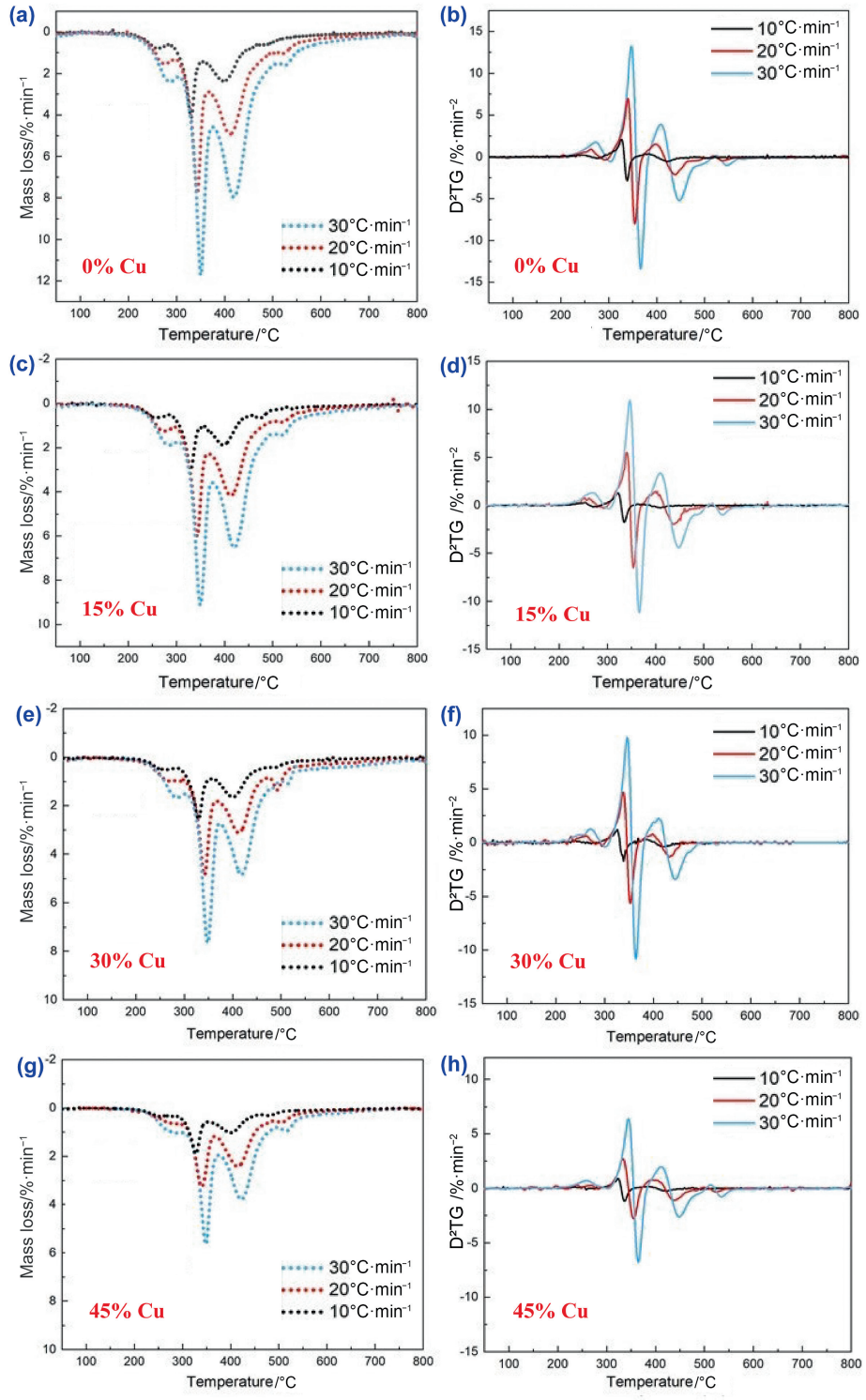

Fig. 3. DTG and D^2TG curves of four resin powders with different copper contents: (a) DTG and (b) D^2TG of resin powder without copper, (c) DTG, and (d) D^2TG of resin powder with a 15% copper mass fraction, (e) DTG and (f) D^2TG resin powder with a 30% copper mass fraction, (g) DTG and (h) D^2TG resin powder with a mass fraction of 45% copper.

$$\frac{d\alpha}{dT} = f(\alpha)\frac{A}{\beta}\exp\left(-\frac{E_a}{RT}\right) \tag{4}$$

At a constant heating rate, β can be expressed by:

$$\beta = \frac{dT}{dt} \tag{5}$$

The FWO method uses the Doyle approximation. Express Eq. (4) in integral and logarithmic form:

$$\ln\ \beta = \ln\frac{AE_\alpha}{RG(\alpha)} - 2.315 - 0.4567\frac{E_\alpha}{RT} \tag{6}$$

Establish the coordinate system of lnβ and $1/T$ and substitute the corresponding points. The slope of the curve under different α values

Table 2
Pyrolysis characteristics of four resin powders with different copper contents

Sample	Heating rate/ °C·min^{-1}	Interval 1	Interval 2	Interval 3	Interval 4	Interval 5	Peak temperature T/°C	Maximum mass loss rate/%·min^{-1}
0	10	220–284	284–353	353–473	473–516	516–800	328	4.13
	20	218–298	298–362	362–494	494–551	551–800	343	7.61
	30	216–303	303–371	371–507	507–574	574–800	351	11.08
15	10	208–284	284–358	358–454	454–521	521–800	329	3.01
	20	218–294	294–365	365–466	466–540	540–800	344	6.13
	30	223–301	301–373	373–494	494–544	544–800	350	9.68
30	10	218–283	283–355	355–440	440–800		329	2.5
	20	221–298	298–363	363–471	471–525	525–800	341	5.11
	30	221–301	301–371	371–490	490–540	540–800	349	7.6
45	10	219–267	267–350	350–449	449–508	508–800	326	1.91
	20	221–300	300–366	366–485	485–533	533–800	341	3.28
	30	222–300	300–373	373–492	492–543	543–800	349	5.62

is obtained by linear fitting, as shown in Fig. 4. Finally, the apparent activation energy under different α values can be calculated.

Table 3 shows the apparent activation energy obtained by simulation calculation for four samples with different copper contents. The data in the table show that the apparent activation energy of the pyrolysis reaction of the resin powder without copper is 133–264 kJ·mol^{-1}, and the apparent activation energy of the pyrolysis reaction of the resin powder containing copper is 93–350 kJ·mol^{-1}. The regression coefficients R^2 of the fitted curves are all greater than 0.97, which can indicate the validity of this set of data.

The apparent activation energy curves of the four resin powder samples with different copper contents are shown in Fig. 5. Several different reaction stages in the pyrolysis process of the sample can be clearly seen in the figure. When $0.1 < \alpha < 0.3$, the corresponding temperature is approximately 290 −350 °C, which exactly corresponds to the temperature of the first transition interval in the TG curve. At this stage, the apparent activation energy showed a significant increase, indicating that a new reaction began to occur at this stage, corresponding to the rapid increase in the mass loss rate in the DTG curve. At this time, the pyrolysis process begins to change from the volatilization of small molecules and the removal of low-bond energy side chains of macromolecules to partial breaks between macromolecular chains. However, it has been observed that the apparent activation energy of copper-containing resin powder is significantly high when $\alpha = 0.3$, while the copper-free resin powder is relatively stable in the range of $0.2 < \alpha < 0.4$ (330 −370 °C). The apparent activation energy of the latter has little change. This indicates that the pyrolysis reaction of the copper-containing resin powder in this range is different from that of the copper-free resin powder. The apparent activation energy of the copper-free resin powder rises steadily in the interval of $0.4 < \alpha < 0.8$, while the apparent activation energy of the copper-containing resin powder begins to rapidly increase when $\alpha = 0.7$. When $\alpha = 0.8$, the activation energy of the copper-containing resin powder exceeds 300 kJ·mol^{-1}, and the resin powder with 15% copper content is close to 350 kJ·mol^{-1}. This value is much higher than the activation energy of the copper-free resin powder at this α value. From the perspective of the entire reaction, the apparent activation energy of the copper-containing resin powder at $0.1 < \alpha < 0.6$ is significantly lower than that of the non-copper resin, and the higher the copper content, the lower the apparent activation energy. The corresponding temperature range of this stage is 280–415 °C, indicating that the activated molecules involved in the reaction have lower activation energy in the copper-containing resin powder at this stage than in the non-copper resin powder. The presence of copper lowers the threshold for chemical reactions in this temperature range and has a certain catalytic effect on the thermal decomposition process at this stage. Copper not only accelerates the reaction rate but also shortens the reaction time. However, as mentioned above, when $\alpha > 0.7$, the apparent activation energy of the copper-containing resin powder rapidly rises and is higher than that of the copper-free resin powder. The corresponding temperature range at this time is 420–520 °C. At this stage, copper may act as a negative catalyst, slowing down the frequency of some chemical reactions and thereby inhibiting the production of some compounds. From the perspective of kinetic analysis, it can be seen from the appearance that the copper content has a certain influence on the entire process of the pyrolysis reaction of the resin powder, but it is impossible to judge whether these effects are beneficial to the pyrolysis of the resin powder. Therefore, we subsequently performed product analysis of the four different copper content samples in the main reaction temperature range to obtain the specific effect of the copper content on the pyrolysis process of the resin powder.

3.3. Discussion of the Py-GC/MS results

Pyrolysis-gas chromatography/mass spectrometry was used to analyze the volatiles produced by four resin powders with different copper contents at different pyrolysis temperatures. The

Table 3
Apparent activation energy and regression coefficient of four different copper content resin powder samples at different α values

Cu	0% Cu		15% Cu		30% Cu		45% Cu	
α	E /kJ·mol^{-1}	R^2	E /kJ·mol^{-1}	R^2	E /kJ·mol^{-1}	R^2	E /kJ·mol^{-1}	R^2
0.1	133.66	0.9915	93.42	0.9970	95.78	0.9807	101.25	0.9722
0.2	158.24	0.9980	133.48	0.9983	136.58	0.9999	135.12	0.9946
0.3	163.34	0.9992	152.42	0.9959	159.70	0.9980	145.68	0.9965
0.4	158.97	0.9921	141.13	0.9801	131.66	0.9798	123.65	0.9701
0.5	175.73	0.9958	167.90	0.9877	161.34	0.9737	139.31	0.9743
0.6	199.76	0.9968	192.66	0.9931	184.29	0.9996	175.18	0.9945
0.7	222.89	0.9945	227.08	0.9972	245.65	0.9985	210.14	0.9991
0.8	263.68	0.9925	349.81	0.9993	318.31	0.9974	324.50	0.9702
0.9	233.45	0.9976	245.29	0.9729	280.98	0.9998	259.49	0.9738

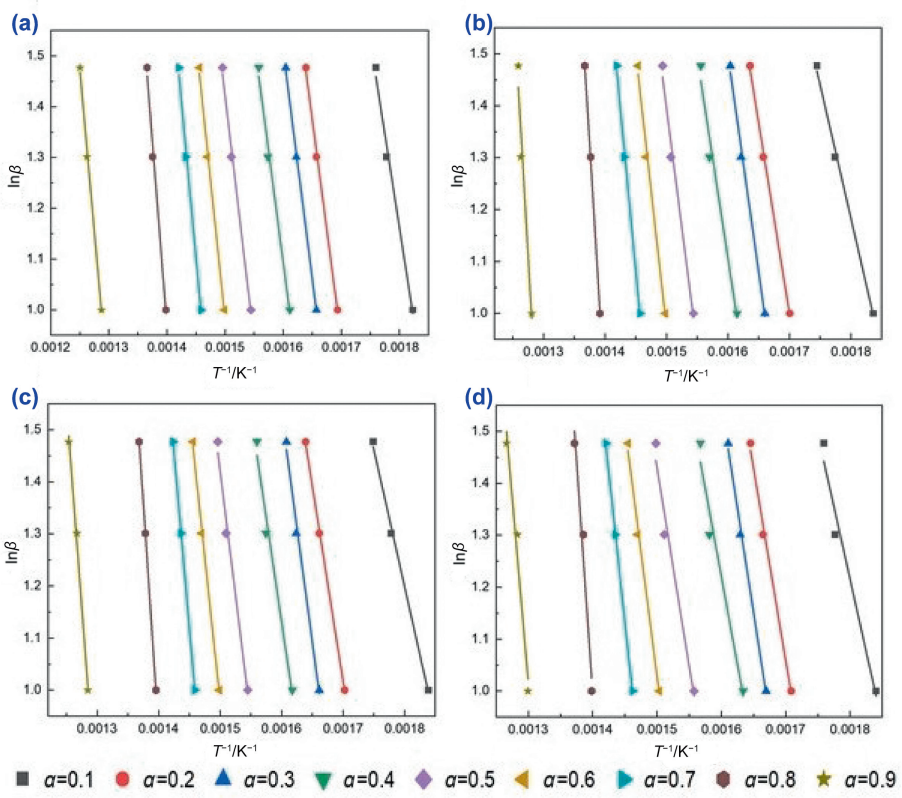

Fig. 4. Linear fitting results of the FWO method for four resin powders with different copper contents under different α values.

temperatures during holding and sampling were 230, 280, 330, 380, 430 and 480 °C. When the detected signal peak and the NIST14 library have a similarity greater than or equal to 90 or the signal peak detected at the same position of samples with different temperatures and copper content matches the same compound multiple times, we believe that the matched molecular structure is reliable. The overlapping chromatograms of four resin powders with different copper contents at different temperatures under the condition of total ion current (TIC) are shown in Fig. 6. The abovementioned figure shows that there are four peaks with larger peak areas in the resin sample, and the corresponding pyrolysis products are phenol, pentanoic acid, erucic acid, and 2-((prop-2-ynyloxy)carbonyl)benzoic acid. The pyrolysis products of resin powder mainly include phenol, substituted phenol (bromo-containing phenol), carbon dioxide, phthalate, triphenyl phosphate (flame retardant), aniline organics and carboxylic acid organics. The abovementioned figure also shows that when the copper content reaches 45%, the number of signal peaks in the mass spectrum is significantly reduced. This result indicates that the types of pyrolysis reaction products are greatly reduced, and it may be that the higher copper content inhibits the formation of some products during the pyrolysis process.

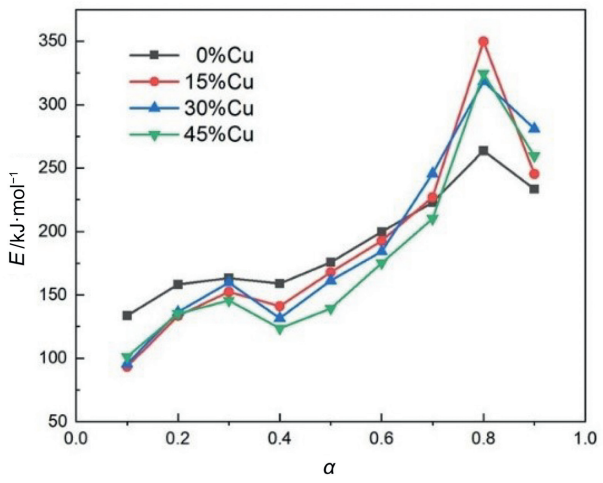

Fig. 5. Apparent activation energy curves of four resin powder samples with different copper contents.

Four samples of resin powder with varying copper concentrations were analyzed for volatile components at various temperatures, and the findings are shown in Table S1 of the Supplementary Material. Combined with the results of thermogravimetric analysis, in the temperature range of the first reaction zone (including the first transition zone) (230–330 °C), the main volatile components are divided into phenol, substituted phenol, carboxyl compounds, phosphorus-containing organics and volatile substance of additives. In the main reaction interval (330–480 °C), in addition to the continuous volatilization of some additives, new compounds appeared one after another such as styrene, substituted anilines, valeric acid, and bromine-containing compounds. The results obtained showed a composition similar to the pyrolysis oil obtained by previous researchers [36]. The pyrolysis resin powder does not seem to escape a large amount of bromine-containing compounds at a lower temperature (not exceeding 300 °C). Resin powder without copper is always the first to detect the presence of bromophenol, and resin powder with 45% copper is only detected to produce 2,4,6-tribromo-phenol at 430 °C. The presence of copper hinders the production of bromine-containing phenol. Even in the presence of excess copper, almost no bromine-containing phenol is formed. It is generally believed that HBr will attack the epoxy unit of the brominated epoxy resin during the pyrolysis process to cause the

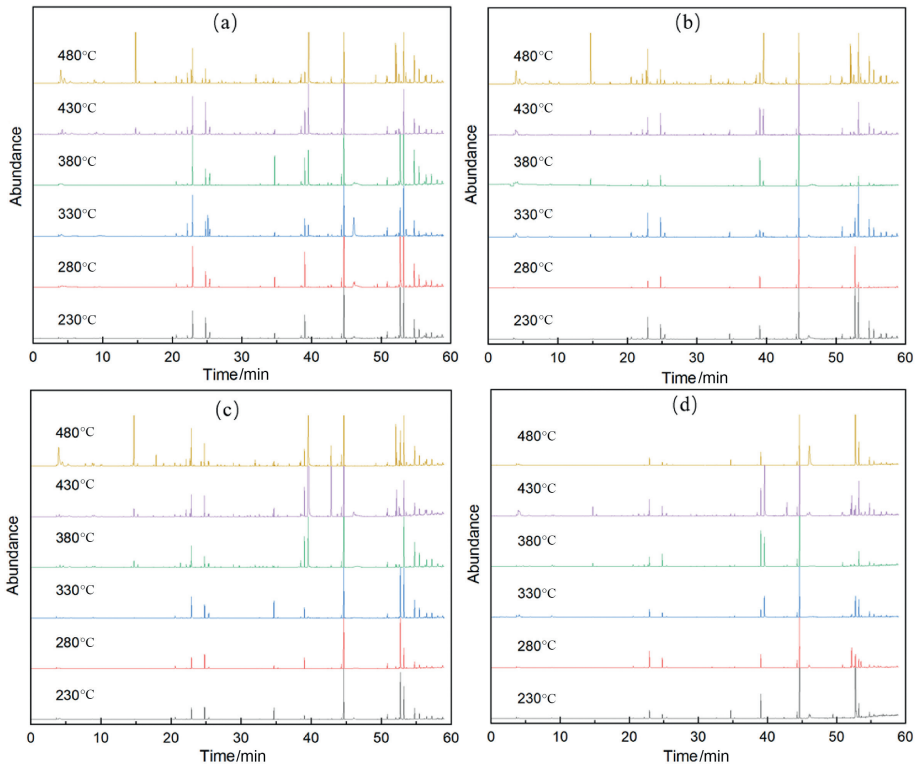

Fig. 6. Ion chromatograms of non-metallic components with different copper contents at 230, 280, 330, 380, 430 and 480 °C: (a) without copper (b) with 10% copper (c) with 20% copper (d) with 30% copper.

release of tetrabromobisphenol A (TBBA) and brominated phenol [37](Fig. 7 Path 1). Combined with the analysis of the apparent activation energy in the previous part, the presence of copper will have a countercatalytic effect in the range of 420–520 °C. It is possible that the presence of copper inhibits the production of bromine-containing phenols. It can be seen from the data in the table that as the copper content increases, this countercatalytic effect becomes more obvious. In addition, it was observed that in the absence of copper, the resin powder would generate aniline during the pyrolysis process, but this product was not detected during the pyrolysis process of the copper-containing resin powder. As shown in Fig. 7 Path 2, the presence of copper may have a fixed effect on the

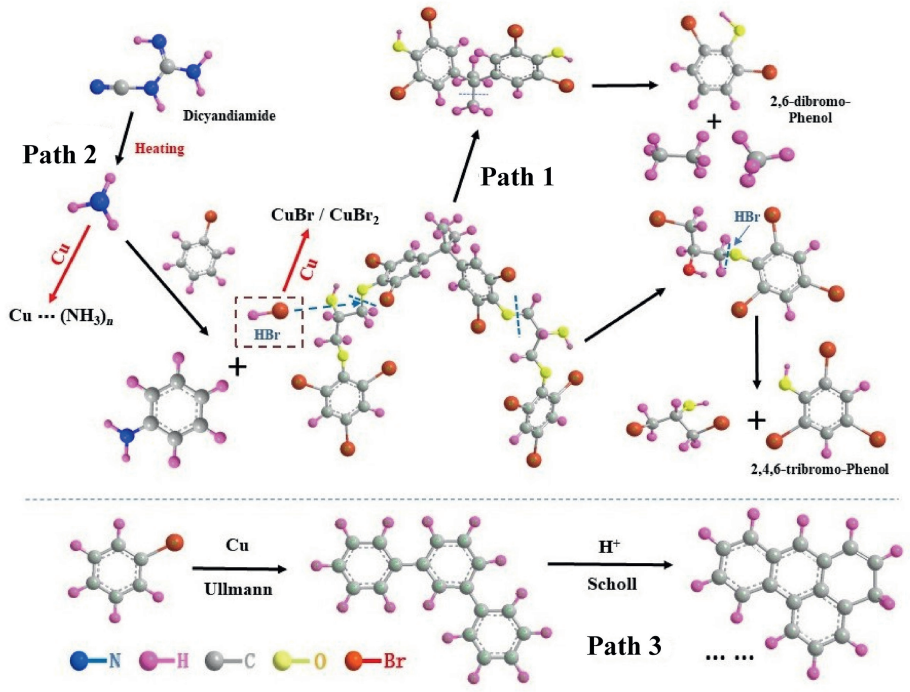

Fig. 7. Possible reaction mechanism during pyrolysis of resin powders. Phthalic acid compounds are not listed one by one due to too many types of substituents.

ammonia produced in the pyrolysis process, which prevents ammonia from reacting with bromine-containing aromatic hydrocarbons to produce aniline and hydrogen bromide. At the same time, excess copper will react with bromine to form copper bromide or cuprous bromide, which will fix the free bromine released during the pyrolysis process in the solid residue. Since the hydrogen bromide concentration in the copper-containing resin powder reaction system is lower than that of the copper-free resin powder, the cracking reaction of macromolecules becomes more difficult. This will cause an increase in the initial reaction temperature of the cleavage and a decrease in the amount of bromine-containing phenol produced. Studies have shown that copper itself has a strong adsorption effect on bromine-containing organics. Excess copper in the reaction system will form a transition complex with bromine-containing organics, which also plays a fixing role for organic bromine [38]. In addition, the presence of copper may cause a Ullmann coupling reaction (Fig. 7 Path 3) in the system and promote the formation of fused ring aromatics in the pyrolysis system.

3.4. Analysis of copper influence mechanism

Calculate the change in bond energy of the circuit board molecule in the presence and absence of copper to learn more about the catalytic mechanism of copper on circuit boards. In this study, Gaussian09 software [39] was used to create molecular models of circuit boards with and without copper. A molecular fragment from Fig. 7 Path 1, which is heavily repeated in the circuit board molecule, was selected for the calculation. Structural optimization and bond energy calculation of molecular fragments of circuit boards with and without copper using the M06-2x method and the 6–311g(d,p) basis set, as shown in Fig. 8. The change in bond energy is shown in Table 4.

The outcomes of the calculations mentioned above. The energy of the majority of bonds decreases with the presence of copper.C6–C7, C7–C8, C7–C9, and C7–C10 are the principal bond-breaking sites, as shown in Fig. 7 Path 1, and their lower bond energies make it simpler for the cleavage of the circuit board molecules to take place. The pyrolysis reaction starts with a reaction involving free radicals. The production of H radicals and Br radicals is facilitated by the decrease in bond energy of other C–H and C–Br bonds, which facilitates the pyrolysis reaction. Moreover, the pyrolysis reaction is made easier by the creation of HBr.

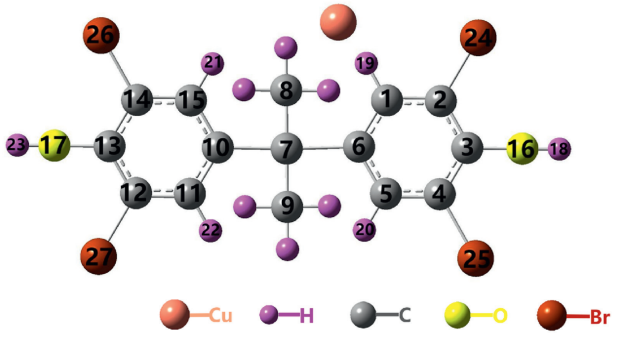

Fig. 8. Circuit board molecular fragment diagram.

Table 4
Value of the change in bond energy of the molecular fragments of the circuit board with or without copper

Bond	ΔBDE(kJ·mol^{-1})	Bond	ΔBDE(kJ·mol^{-1})
C7–C6	−81.62	C15–H21	−43.65
C7–C8	−150.84	C11–H22	−265.65
C7–C9	−153.92	O16–H18	−188.22
C7–C10	−81.59	O17–H23	−44.59
C3–O16	−143.03	C2–Br24	−274.88
C13–O17	+9.30	C4–Br25	−267.20
C1–H19	−283.29	C14–Br26	+19.96
C5–H20	−288.21	C12–Br27	+46.59

4. Conclusions

The primary purpose of this study was to investigate the effects of copper content on the pyrolysis of discarded circuit board nonmetallic resin powder using the combination of TG and Py-GC/MS. The pyrolysis of resin samples occurs in three primary stages, as determined by thermogravimetric analysis. The first stage is mainly the volatilization of low-boiling small molecules and the removal of large molecular side chains. The second stage is the main reaction zone for the cleavage of organic matter, which is manifested in the breaking of macromolecular structural bonds, intermolecular condensation, and the formation of bromine-containing organics. The presence of copper shortens the reaction time and temperature range at this stage. The third stage mainly involves the deep carbonization of residual carbon and the continuous escape of some residual small molecules. With rising temperature, the total degree of the reaction frequently becomes complete. The catalytic effect of copper on low-temperature reactions and its counter-catalytic effect on the primary reaction are the two main ways in which copper has an impact on the pyrolysis reaction of resin samples. Copper lowers the reaction's apparent activation energy during the low-temperature stage and speeds up the reaction rate. In addition, copper inhibits the formation of bromine-containing compounds by reacting with ammonia to form a copper ammonia complex and fixing bromine in the reaction system to form cuprous bromide. With rising copper content, this inhibitory effect keeps growing. Moreover, the presence of copper lowers the bonding energy of the majority of the molecules on the circuit board, making it simpler for the molecules to split. This study has added to the basic research and mechanistic understanding of bromide pyrolysis.

Declaration of Interest

The authors declare that they have no known competing financial interests or personal relationships that could have appeared to influence the work reported in this paper.

CRediT Authorship Contribution Statement

Bin Li: Conceptualization, Funding acquisition, Methodology, Project administration, Resources, Writing – original draft, Writing – review & editing. Biqin Shen: Data curation, Formal analysis, Investigation, Validation, Writing – original draft, Writing – review & editing. Ran Tao: Supervision, Writing – review & editing. Chenwei Hu: Writing – review & editing. Yufeng Wu: Conceptualization, Funding acquisition, Project administration, Supervision, Writing – review & editing, Writing – original draft. Haoran Yuan: Investigation, Resources, Supervision. Jing Gu: Supervision, Validation. Yong Chen: Supervision, Validation.

Acknowledgements

This work was supported by the National Key Research and Development Program of China (2018YFC1902504).

Supplementary Material

Supplementary data to this article can be found online at https://doi.org/10.1016/j.cjche.2024.04.024.

References

[1] M. Kaya, Recovery of metals and nonmetals from electronic waste by physical and chemical recycling processes, *Waste Manag.* 57 (2016) 64–90.
[2] M. Sharma, D. Kaushal, S. Joshi, A. Kumar, Electronic waste disposal behavioral intention of millennials: a moderating role of electronic word of mouth (eWOM) and perceived usage of online collection portal, *J. Clean. Prod.* 447 (2024) 141121.
[3] J.J. Chen, B. Li, D. Yu, D. Pan, T.Y. Zuo, Status analysis on recycling technology of spent printed circuit board, *Mod. Chem. Ind.* 39 (5) (2019) 42–46.
[4] A.A. Aboud, A. Mukherjee, N. Revaprasadu, The effect of Cu-doping on CdS thin films deposited by the spray pyrolysis technique, *J. Mater. Res. Technol.* 8 (2) (2019) 2021–2030.
[5] R. Gao, L. Zhan, J. Guo, Z. Xu, Research of the thermal decomposition mechanism and pyrolysis pathways from macromonomer to small molecule of waste printed circuit board, *J. Hazard Mater.* 383 (2020) 121234.
[6] R. Jujun, Z. Jie, H. Jian, J. Zhang, A novel designed bioreactor for recovering precious metals from waste printed circuit boards, *Sci. Rep.* 5 (1) (2015) 13481.
[7] R. Qiu, M. Lin, B. Qin, Z. Xie, Environmental-friendly recovery of non-metallic resources from waste printed circuit boards: a review, *J. Clean. Prod.* 279 (2021) 123738.
[8] M. Arabiourrutia, G. Lopez, M. Artetxe, J. Alvarez, J. Bilbao, Waste tyre valorization by catalytic pyrolysis – a review, *Renew. Sustain. Energy Rev.* 129 (2020) 109932.
[9] D. Lee, J. Lu, J. Chang, Pyrolysis synergy of municipal solid waste (MSW): a review, *Bioresour. Technol.* 318 (2020) 123912.
[10] B. Li, R. Tao, Y. Wu, W. Zhang, X. Liu, W. Wang, Study on the pyrolysis characteristics and reaction mechanisms of WLED packaging materials, *J. Anal. Appl. Pyrol.* 170 (2023) 105935.
[11] Y. Kim, T.U. Han, S. Kim, J. Jae, J. Jeon, Y. Park, Catalytic co-pyrolysis of epoxy-printed circuit board and plastics over HZSM-5 and HY, *J. Clean. Prod.* 168 (2017) 366–374.
[12] B. Liu, R. Gao, Z. Xu, Fabrication of super-hydrophobic surfaces utilizing pyrolysis of waste printed circuit boards, *J. Clean. Prod.* 244 (2020) 118727.
[13] Y. Kim, T.U. Han, C. Watanabe, N. Teramae, S. Kim, B. Huang, Analytical pyrolysis of waste paper laminated phenolic-printed circuit board (PLP-PCB), *J. Anal. Appl. Pyrol.* 115 (2015) 87–95.
[14] C. Li, H. Xia, C. Liu, K. Zeng, Analysis of the effect of heating rate on pyrolysis kinetics and product composition of copper-containing waste circuit boards, *Environ. Sci. Pollut. Control Ser.* 30 (12) (2023) 33075–33089.
[15] N. Ortuño, J. Moltó, S. Egea, R. Font, Thermogravimetric study of the decomposition of printed circuit boards from mobile phones, *J. Anal. Appl. Pyrol.* 103 (2013) 189–200.
[16] N. Du, H. Ma, H. Zhang, F. Yang, Simulation study on the heat transfer characteristics of a single printed circuit board particle in the pyrolysis process, *Fuel Process. Technol.* 192 (2019) 45–56.
[17] X. Du, L. Wang, W. Zhao, Y. Wang, T. Qi, Preparation of hierarchical porous carbon from waste printed circuit boards for high performance electric double-layer capacitors, *J. Power Sources* 323 (2016) 166–173.
[18] H. Chiang, K. Lin, M. Lai, T. Chen, Pyrolysis characteristics of integrated circuit boards at various particle sizes and temperatures, *J. Hazard Mater.* 149 (1) (2007) 151–159.
[19] C. Zhao, X. Zhang, L. Shi, Catalytic pyrolysis characteristics of scrap printed circuit boards by TG-FTIR, *Waste Manag.* 61 (2017) 354–361.
[20] G. Jie, L. Ying-Shun, L. Mai-Xi, Product characterization of waste printed circuit board by pyrolysis, *J. Anal. Appl. Pyrol.* 83 (2) (2008) 185–189.
[21] Q. Deng, D. Pan, G. Liu, F. Yang, J. Pan, Leaching Br from high bromine containing circuit board smelting flue dust by sodium hydroxide solution: thermodynamics and kinetics study, *J. Mater. Res. Technol.* 9 (4) (2020) 8675–8684.
[22] C. Li, H. Xia, C. Liu, K. Zeng, Steam gasification assisted pyrolysis directional de bromination of waste printed circuit boards and comprehensive utilization of products, *J. Clean. Prod.* 366 (2022) 132979.
[23] R. Wang, Z. Zhu, S. Tan, J. Guo, Z. Xu, Mechanochemical degradation of brominated flame retardants in waste printed circuit boards by Ball Milling, *J. Hazard Mater.* 385 (2020) 121509.
[24] T. Zhang, X. Mao, J. Qu, Y. Liu, Microwave-assisted catalytic pyrolysis of waste printed circuit boards, and migration and distribution of bromine, *J. Hazard Mater.* 402 (2021) 123749.
[25] J. Zhu, X. Chen, N. Zhao, W. Wei, J.D. Chen, Bromine removal from resin particles of crushed waste printed circuit boards by vacuum low-temperature heating, *J. Clean. Prod.* 262 (2020) 121390.
[26] C. Ma, T. Kamo, Two-stage catalytic pyrolysis and debromination of printed circuit boards: effect of zero-valent Fe and Ni metals, *J. Anal. Appl. Pyrol.* 134 (2018) 614–620.
[27] O. Terakado, R. Ohhashi, M. Hirasawa, Bromine fixation by metal oxide in pyrolysis of printed circuit board containing brominated flame retardant, *J. Anal. Appl. Pyrol.* 103 (2013) 216–221.
[28] R. Gao, B. Liu, L. Zhan, J. Guo, Z. Xu, Catalytic effect and mechanism of coexisting copper on conversion of organics during pyrolysis of waste printed circuit boards, *J. Hazard Mater.* 403 (2021) 123465.
[29] W. Liu, J. Xu, J. Han, F. Qin, Z. Zhang, Kinetic and mechanism studies on pyrolysis of printed circuit boards in the absence and presence of copper, *ACS Sustain. Chem. Eng.* 7 (2) (2018) 1879–1889.
[30] L. Qin, J. Han, B. Zhao, Y. Wang, F. Xing, Thermal degradation of medical plastic waste by *in-situ* FTIR, TG-MS and TG-GC/MS coupled analyses, *J. Anal. Appl. Pyrol.* 136 (2018) 132–145.
[31] F. Mustata, N. Tudorachi, Thermal behavior of epoxy resin cured with aromatic dicarboxylic acids, *J. Therm. Anal. Calorim.* 125 (1) (2016).
[32] I. de Marco, B.M. Caballero, M.J. Chomón, Pyrolysis of electrical and electronic wastes, *J. Anal. Appl. Pyrol.* 82 (2) (2008) 179–183.
[33] P. Parthasarathy, A. Fernandez, T. Al-Ansari, H. Mackey, Thermal degradation characteristics and gasification kinetics of camel manure using thermogravimetric analysis, *J. Environ. Manag.* 287 (2021) 112345.
[34] N. Masawat, D. Atong, V. Sricharoenchaikul, Thermo-kinetics and product analysis of the catalytic pyrolysis of Pongamia residual cake, *J. Environ. Manag.* 242 (2019) 238–245.
[35] O. Takeo, Non-isothermal kinetics and generalized time, *Thermochi Acta.* 100 (1) (1986).
[36] R. Cao, R. Zhou, Y. Liu, W. Wei, Z. Nan, Research on the pyrolysis characteristics and mechanisms of waste printed circuit boards at fast and slow heating rates, *Waste Manag* 149 (2022) 134–145.
[37] H. Kaya, J. Hacaloglu, Thermal degradation of polystyrene composites. Part I. The effect of brominated polyepoxy and antimony oxid, *J. Anal. Appl. Pyrol.* 105 (2014) 301–308.
[38] L. Ming, G. Shun, W. Zhiying, L.H. Zhu, H. Tang, Ultrarapid and deep debromination of tetrabromodiphenyl ether over noble-metal-free Cu/TiO_2 nanocomposites under mild conditions, *Environ. Sci. Technol.* 52 (20) (2018).
[39] M.J. Frisch, G.W. Trucks, H.B. Schlegel, G.E. Scuseria, M.A. Robb, J.R. Cheeseman, G. Scalmani, V. Barone, B. Mennucci, G.A. Petersson, H. Nakatsuji, M. Caricato, X. Li, H.P. Hratchian, A.F. Izmaylov, J. Bloino, G. Zheng, J.L. Sonnenberg, M. Hada, M. Ehara, K. Toyota, R. Fukuda, J. Hasegawa, M. Ishida, T. Nakajima, Y. Honda, O. Kitao, H. Nakai, T. Vreven, J.A. Montgomery Jr., J.E. Peralta, F. Ogliaro, M. Bearpark, J.J. Heyd, E. Brothers, K.N. Kudin, V.N. Staroverov, R. Kobayashi, J. Normand, K. Raghavachari, A. Rendell, J.C. Burant, S.S. Iyengar, J. Tomasi, M. Cossi, N. Rega, J.M. Millam, M. Klene, J.E. Knox, J.B. Cross, V. Bakken, C. Adamo, J. Jaramillo, R. Gomperts, R.E. Stratmann, O. Yazyev, A.J. Austin, R. Cammi, C. Pomelli, J.W. Ochterski, R.L. Martin, K. Morokuma, V.G. Zakrzewski, G.A. Voth, P. Salvador, J.J. Dannenberg, S. Dapprich, A.D. Daniels, Ö. Farkas, J.B. Foresman, J.V. Ortiz, J. Cioslowski, D.J. Fox, Gaussian 09, Gaussian, Inc, Wallingford, CT, 2009.